

Functional Characterization of Mammalian Inositol 1,4,5-Trisphosphate Receptor Isoforms

Huiping Tu,* Zhengnan Wang,* Elena Nosyreva,* Humbert De Smedt,[†] and Ilya Bezprozvanny*

*Department of Physiology, University of Texas Southwestern Medical Center at Dallas, Dallas, Texas 75390 USA; and

[†]Laboratorium voor Fysiologie, K.U.Leuven, B-3000, Leuven, Belgium

ABSTRACT Inositol 1,4,5-trisphosphate receptors (InsP₃R) play a key role in intracellular calcium (Ca²⁺) signaling. Three mammalian InsP₃R isoforms—InsP₃R type 1 (InsP₃R1), InsP₃R type 2 (InsP₃R2), and InsP₃R type 3 (InsP₃R3) are expressed in mammals, but the functional differences between the three mammalian InsP₃R isoforms are poorly understood. Here we compared single-channel behavior of the recombinant rat InsP₃R1, InsP₃R2, and InsP₃R3 expressed in Sf9 cells, reconstituted into planar lipid bilayers and recorded with 50 mM Ba²⁺ as a current carrier. We found that: 1), for all three mammalian InsP₃R isoforms the size of the unitary current is 1.9 pA and single-channel conductance is 74–80 pS; 2), in optimal recording conditions the maximal single-channel open probability for all three mammalian InsP₃R isoforms is in the range 30–40%; 3), in optimal recording conditions the mean open dwell time for all three mammalian InsP₃R isoforms is 7–8 ms, the mean closed dwell time is ~10 ms; 4), InsP₃R2 has the highest apparent affinity for InsP₃ (0.10 μM), followed by InsP₃R1 (0.27 μM), and then by InsP₃R3 (0.40 μM); 5), InsP₃R1 has a high-affinity (0.13 mM) ATP modulatory site, InsP₃R2 gating is ATP independent, and InsP₃R3 has a low-affinity (2 mM) ATP modulatory site; 6), ATP modulates InsP₃R1 gating in a noncooperative manner ($n_{\text{Hill}} = 1.3$); 7), ATP modulates InsP₃R3 gating in a highly cooperative manner ($n_{\text{Hill}} = 4.1$). Obtained results provide novel information about functional properties of mammalian InsP₃R isoforms.

INTRODUCTION

The inositol (1,4,5)-trisphosphate receptor (InsP₃R) is an intracellular calcium (Ca²⁺) release channel that plays a key role in Ca²⁺ signaling in cells (Berridge, 1993). Three InsP₃R isoforms—InsP₃R type 1 (InsP₃R1), InsP₃R type 2 (InsP₃R2), and InsP₃R type 3 (InsP₃R3) are expressed in mammals (Furuichi et al., 1994), each with a unique expression pattern. InsP₃R1 is predominant in the central nervous system, but most other tissues express at least two and often all three InsP₃R isoforms at different ratios (Taylor et al., 1999). The InsP₃R is a large (~1 MDa) tetrameric complex (Furuichi et al., 1994). The three mammalian InsP₃R isoforms are 60–70% identical in sequence (Furuichi et al., 1994) and share a common domain structure (Mignery and Sudhof, 1990; Miyawaki et al., 1991) that consists of an amino-terminal InsP₃-binding domain, a carboxy-terminal Ca²⁺ channel domain, and a middle coupling domain containing most of the putative regulatory sites. The InsP₃-binding and Ca²⁺ channel-forming domains are highly conserved between InsP₃R isoforms, whereas the middle coupling domain is the most divergent.

Functional properties of native and recombinant InsP₃R1 have been extensively characterized by Ca²⁺ flux measurements, planar lipid bilayer or nuclear envelope patch-clamp recordings (reviewed in Bezprozvanny and Ehrlich, 1995; Thrower et al., 2001). In contrast with InsP₃R1, functional properties of InsP₃R2 and InsP₃R3 are less known (Thrower

et al., 2001). The functional properties of purified native cardiac InsP₃R2 (Ramos-Franco et al., 1998), purified recombinant InsP₃R2 expressed in COS cells (Ramos-Franco et al., 2000), and native InsP₃R3 from RINm5F cells (Hagar et al., 1998; Hagar and Ehrlich, 2000) were characterized in planar lipid bilayers. The functional properties of recombinant InsP₃R3 expressed in *Xenopus* oocytes were described in nuclear envelope patch-clamp experiments (Mak et al., 2001a,b, 2000). Some of these studies resulted in conflicting data, but because of differences in techniques, experimental conditions and expression systems used by various groups, systematic comparison of obtained results is difficult.

Ca²⁺ signals supported by different endogenous chicken InsP₃R isoforms have been previously compared in a Ca²⁺ imaging study with genetically altered DT40 cells by systematically deleting two out of three isoforms (Miyakawa et al., 1999). In the latter approach, however, comparison of functional properties of the three InsP₃R isoforms is complicated by the differences in the endogenous expression levels of each isoform in DT40 cells. To compare single-channel properties of mammalian InsP₃R isoforms in identical conditions, here we expressed rat InsP₃R1, InsP₃R2, and InsP₃R3 in *Spodoptera frugiperda* (Sf9) cells. The recombinant InsP₃R isoforms were reconstituted into planar lipid bilayers and characterized in identical recording conditions using 50 mM Ba²⁺ as a current carrier. The Ca²⁺ imaging results obtained in DT40 cells (Miyakawa et al., 1999) formed a framework for interpretation of single-channel data with different InsP₃R isoforms obtained in our experiments. Our results provide a first comprehensive

Submitted July 14, 2004, and accepted for publication October 29, 2004.

Address reprint requests to Dr. Ilya Bezprozvanny, Dept. of Physiology, K4.112 UT Southwestern Medical Center at Dallas, 5323 Harry Hines Blvd., Dallas, TX 75390-9040. Tel.: 214-648-6737; Fax: 214-648-2974; E-mail: Ilya.bezprozvanny@utsouthwestern.edu.

© 2005 by the Biophysical Society

0006-3495/05/02/1046/10 \$2.00

doi: 10.1529/biophysj.104.049593

description of single-channel properties of the three mammalian InsP₃R isoforms in identical experimental conditions.

MATERIALS AND METHODS

Generation of recombinant baculoviruses

The baculoviruses expressing rat InsP₃R1 (RT1) and rat InsP₃R3 (RT3) have been previously described (Maes et al., 2000; Tu et al., 2002). To generate rat InsP₃R2-encoding baculovirus (RT2) a coding sequence of rat InsP₃R2 in pCMV5 vector (Ramos-Franco et al., 2000; Sudhof et al., 1991) was subcloned into pFastBac1 vector (Invitrogen, Carlsbad, CA) and 5' untranslated region (UTR) was replaced with the Kozak sequence by PCR using the *Bss*HII (5' UTR) and *Sfi*I (2143) restriction sites. The RT2 baculoviruses were generated and amplified using the Bac-to-Bac system according to the manufacturer's (Invitrogen) instructions.

Expression of InsP₃R in Sf9 cells

S. frugiperda (Sf9) cells were obtained from American Type Culture Collection (Manassas, VA) and cultured in suspension culture in supplemented Grace's insect media (Invitrogen) with 10% fetal bovine serum at 27°C. The three isoforms of InsP₃R (RT1, RT2, and RT3) were expressed in Sf9 cells as previously described for RT1 (Nosyreva et al., 2002; Tu et al., 2002). Briefly, 150 ml of Sf9 cell culture was infected by InsP₃R-encoding baculoviruses at multiplicity of infection (MOI) of 5–10. Sf9 cells were collected 66–72 h postinfection by centrifugation at 4°C for 5 min at 800 rpm (GH 3.8 rotor, Beckman Instruments, Fullerton, CA). The cellular pellet was resuspended in 25 ml of homogenization buffer A (0.25 M sucrose, 5 mM Hepes, pH 7.4) supplemented with protease inhibitors cocktail (1 mM EDTA, aprotinin 2 µg/ml, leupeptin 10 µg/ml, benzamide 1 mM, 4-(2-aminoethyl)-benzenesulfonyl fluoride hydrochloride 2.2 mM, pepstatin 10 µg/ml, phenylmethylsulfonyl fluoride 0.1 mg/ml). Cells were disrupted by sonication (Branson Ultrasonics, Danbury, CT) and manually homogenized on ice with a glass-Teflon homogenizer.

The microsomes were isolated from the Sf9 cell homogenate by differential centrifugation as previously described (Kaznatcheyeva et al., 1998). Briefly, 25 ml of Sf9 cell homogenate was centrifuged for 15 min at 4 k g_{max} (J 25.50 rotor, Beckman Instruments). The supernatant fluid was filtered through cheese cloth, and the filtrate was centrifuged for 30 min at 90 k g_{max} (Ti 50.2 rotor, Beckman Instruments). The pellet from the latter spin was resuspended in 25 ml of high-salt buffer B (0.6 M KCl, 5 mM Na₂SO₄, 20 mM Na₄P₂O₇, 1 mM EDTA, 10 mM HEPES, pH 7.2) and manually homogenized on ice using Teflon/glass manual homogenizer and centrifuged for 15 min at 4 k g_{max} (J 25.50 rotor, Beckman Instruments). The resulting supernatant fluid was centrifuged for 30 min at 90 k g_{max} (Ti 50.2 rotor, Beckman Instruments). The pellet from the last spin was resuspended in 0.5 ml of the storage buffer (10% sucrose, 10 mM 3-morpholinopropanesulfonic acid, pH 7.0) to typically yield 6 mg/ml of protein (Bradford assay, Bio-Rad), aliquoted, quickly frozen in liquid nitrogen, and stored at –80°C.

Expression of InsP₃R isoforms was confirmed by Western blotting with isoform-specific antibodies. Rabbit polyclonal anti-InsP₃R1 antibody T443 was previously described (Kaznatcheyeva et al., 1998). Rabbit polyclonal anti-InsP₃R2 (IB7122) and anti-InsP₃R3 (IB7124) antibodies were generated against keyhole limpet haemocyanin-conjugated InsP₃R2 (RLGFLGSNTPHENHHMPPH) and InsP₃R3 (RLGFVDVQNCMSR) carboxy-terminal peptides and affinity purified (AP) on antigenic peptides conjugated to *N*-hydroxysuccinimide-activated Sepharose (Amersham-Pharmacia Biotech).

Single-channel recordings of InsP₃R activity

Planar lipid bilayers were formed from dioleoyl-phosphoethanolamine/dioleoyl-phosphoserine (3:1) synthetic lipid (Avanti Polar Lipids, Alabaster,

AL) mixture in decane on the small (100–200 µm in diameter) hole in Teflon film separating two chambers 3 ml each (*cis* and *trans*). Before formation of the bilayer the hole was prepatented with phytanoyl-phosphocholine/dioleoyl-phosphoserine (3:1) synthetic lipid (Avanti Polar Lipids) mixture in decane. Recombinant InsP₃R isoforms were incorporated into planar lipid bilayers by microsomal vesicle fusion as described previously for the wild-type and mutant InsP₃R1 (Nosyreva et al., 2002; Tu et al., 2002). In these experiments endoplasmic reticulum (ER) microsomes were added to the *cis* chamber with stirring, and fusion of microsomes to the bilayer was induced by osmotic pressure resulting from an addition of 0.6–1 M KCl to the *cis* chamber. Fusion of ER microsomes to the bilayer leads to incorporation of the channels in such an orientation that the *cis* side is equivalent to cytosol and the *trans* side is equivalent to the lumen of ER (Miller, 1986). Fusion of ER vesicles with the bilayer was registered by the appearance of chloride currents. Once sufficient fusion was achieved (>100 pA of chloride currents), *cis* chamber (cytosolic) was perfused with 20 vol of *cis* recording solution (110 mM Tris dissolved in HEPES, pH 7.35) with stirring. The *trans* chamber (luminal) was filled with *trans* recording solution (50 mM Ba(OH)₂ dissolved in HEPES, pH 7.35), leaving 50 mM Ba²⁺ as a main charge carrier (Bezprozvanny and Ehrlich, 1994). The *cis* chamber was held at virtual ground and the *trans* chamber was voltage clamped (Warner OC-725C bilayer clamp) in the range of membrane potentials (*cis* chamber potential relative to *trans* chamber potential) from +10 to –30 mV as indicated in the text. The liquid junction potential between *cis* and *trans* recording solutions was compensated before formation of the bilayer.

The InsP₃R single-channel currents were amplified (Warner OC-725C), filtered at 1 kHz by low-pass eight-pole Bessel filter (model 900, Frequency Devices, Haverhill, MA), digitized at 5 kHz (Digidata 1200, Axon Instruments, Union City, CA), stored on a computer hard drive and recordable optical disks, and analyzed offline using pClamp 6 (Axon Instruments) and WinEDR V2.3 (Dempster, 2001). For single-channel analysis currents were filtered digitally at 500 Hz, and for presentation of the current traces data were filtered at 200 Hz. All-points amplitude histograms were generated from current records at least 100-s long and fit by a sum of two Gaussian functions (WinEDR V2.3). Channel openings were detected by half-threshold ($t \geq 2$ ms) crossing criteria (Sakmann and Neher, 1983) using pClamp 6. We have not corrected for missed events in our analysis. Open and closed dwell-time distributions were fit by a single exponential fit (pClamp 6).

InsP₃- and ATP-dependence of InsP₃R was determined as described in (Bezprozvanny and Ehrlich, 1993; Lupu et al., 1998) by consecutive additions to the *cis* chamber from the concentrated stocks (1 mM InsP₃ or 100 mM and 500 mM Na₂ATP) with at least 30 s stirring of solutions in both chambers. Evidence for the presence of multiple channels in the bilayer (multiple open levels) was obtained in the majority of the experiments. The number of active channels in the bilayer was estimated as a maximal number of simultaneously open channels during the course of an experiment (Horn, 1991). The probability of the closed level, and first and second open levels was determined by using half-threshold crossing criteria ($t \geq 2$ ms) from the records lasting at least 100 s at each InsP₃ or ATP concentrations. The single-channel open probability (P_o) was calculated using the binomial distribution for the levels 0, 1, and 2, and assuming that the channels in the bilayer were identical and independent (Colquhoun and Hawkes, 1983). Potential errors of absolute P_o values associated with the possible underestimate of the number of active channels in the bilayer were minimized by normalizing the P_o to the maximum P_o observed in the same experiment. The normalized data from several experiments with each InsP₃R isoform were averaged together for presentation and fitting. The fits were generated using least-squares routine (SigmaPlot 2001, Jandel Scientific, San Rafael, CA) and the quality of the fit was evaluated from the coefficient of determination (R^2). The standard errors of resulting parameters were obtained as the estimates of the uncertainties in the values of regression coefficients obtained as a result of the fitting procedure (SigmaPlot 2001, Jandel Scientific).

To obtain the parameters of InsP₃ dependence, the normalized and averaged data were fit by the equation

$$P[InsP_3] = P_m [InsP_3]^n / (k_{InsP_3}^n + [InsP_3]^n), \quad (1)$$

modified from Lupu et al. (1998), where P_m is the maximal normalized open probability, n is the Hill coefficient, and k_{InsP_3} is the apparent affinity for $InsP_3$.

To obtain the parameters of ATP dependence, the normalized and averaged data were fit by the equation

$$P[ATP] = P_0 + P_m [ATP]^n / (k_{ATP}^n + [ATP]^n), \quad (2)$$

modified from Bezprozvanny and Ehrlich (1993), where P_0 is the normalized open probability in the absence of ATP, P_m is the maximal increase in normalized P_0 induced by ATP, n is the Hill coefficient, and k_{ATP} is the apparent affinity for ATP.

RESULTS

Expression and functional properties of mammalian $InsP_3R$ isoforms

The baculoviruses encoding rat $InsP_3R1$ (RT1) and rat $InsP_3R3$ (RT3) have been previously described (Maes et al., 2000; Tu et al., 2002). The baculovirus encoding rat $InsP_3R2$ (RT2) has been generated as described in Materials and Methods. The *S. frugiperda* (Sf9) cells infected with RT1, RT2, and RT3 baculoviruses were used to prepare microsomes 66–72 h postinfection as described in Materials and Methods. The microsomes prepared from noninfected Sf9 cells (Sf9) and from RT1-, RT2-, or RT3-infected Sf9 cells were analyzed by Western blotting with anti- $InsP_3R1$ T443 antibodies (Fig. 1 A), anti- $InsP_3R2$ affinity purified IB7122-AP antibodies (Fig. 1 B), and anti- $InsP_3R3$ affinity purified IB7124-AP antibodies (Fig. 1 C). A prominent immunoreactive band of ~260 kDa was detected in samples from baculovirus-infected cells, but not in noninfected control samples (Fig. 1, A–C). The specificity of the isoform-specific $InsP_3R$ antibodies used in these experiments is supported by the lack of cross-reactivity with microsomes from RT1, RT2, and RT3-infected Sf9 cells (Fig. 1, A–C). Our results support efficient expression of full-length rat $InsP_3R1$, $InsP_3R2$, and $InsP_3R3$ in RT1-, RT2-, and RT3-infected Sf9 cells in our experimental conditions.

As we previously described (Nosyreva et al., 2002; Tu et al., 2002, 2003), when the microsomes isolated from RT1-infected Sf9 cells were fused with planar lipid bilayers, $InsP_3$ -gated channel activity was frequently (60/70) observed (Fig. 2 A). In contrast, the $InsP_3$ -gated channels were never ($n = 10$) observed in the experiments with microsomes isolated from uninfected Sf9 cells (Nosyreva et al., 2002; Tu et al., 2002, 2003). Similar to experiments with microsomes from RT1-infected Sf9 cells, $InsP_3$ -gated channels were frequently observed in experiments with microsomes from RT2-infected Sf9 cells (35/40) (Fig. 3 A) and with microsomes from RT3-infected Sf9 cells (40/46) (Fig. 4 A). Most of the experiments with microsomes from RT1-, RT2-, and RT3-infected Sf9 cells resulted in incorporation of multiple active $InsP_3R$ in the bilayer. To compare the basic channel properties of recombinant $InsP_3R1$, $InsP_3R2$, and $InsP_3R3$ we performed single-channel analysis of currents recorded in a few experiments with only a single active $InsP_3R$ in the bilayer for each

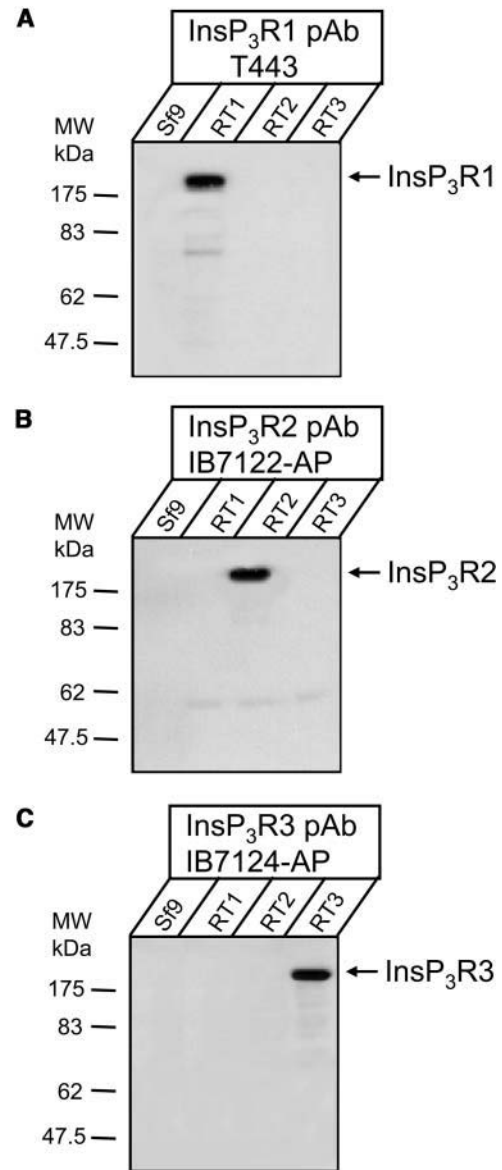


FIGURE 1 Expression of mammalian $InsP_3R$ isoforms in Sf9 cells. Western blot of microsomal proteins. Microsomes isolated from noninfected Sf9 cells (Sf9) and from Sf9 cells infected with RT1, RT2, and RT3 baculoviruses were analyzed by Western blotting with polyclonal antibodies specific for $InsP_3R1$ (A), $InsP_3R2$ (B), and $InsP_3R3$ (C) as indicated. For each microsomal preparation, 10 μ g of total protein was loaded on the gel.

$InsP_3R$ isoform (as judged by the absence of multiple open levels). From this analysis we determined that in standard recording conditions (pCa 6.7, 0.5 mM ATP, 2 μ M $InsP_3$), $InsP_3R1$ and $InsP_3R2$ displayed similar levels of activity with P_0 values of ~30% (Figs. 2 A and 3 A; Table 1). In contrast, $InsP_3R3$ channels were less active in standard recording conditions, with P_0 values <5% (Fig. 4 A; Table 1).

All-points current amplitude histograms for each $InsP_3R$ isoform were fit by a sum of two Gaussian functions corresponding to the closed and open states of the channels

(panel *B* in Figs. 2–4). Thus, all three InsP₃R isoforms open primarily to the main conductance state and subconductance states (Watrás et al., 1991) are infrequent. At 0 mV holding potential, the size of the unitary current for the main conductance state of all 3 InsP₃R isoforms in our experimental conditions was close to 1.9 pA (Figs. 2 *B*, 3 *B*, and 4 *B*; Table 1). The open dwell time distribution was fit by a single exponential function (Figs. 2 *C* and 3 *C*) with the mean open time in the range 7–8 ms for InsP₃R1 and InsP₃R2 isoforms (Table 1). The dwell closed time distribution was also fit by a single exponential function (Figs. 2 *D* and 3 *D*) with the mean closed time close to 10 ms for InsP₃R1 and InsP₃R2 (Table 1). Because of the low frequency of openings (Fig. 4), we were not able to collect enough events to perform kinetic analysis of InsP₃R3 channels in standard recording conditions. To further characterize the conductance properties of three mammalian InsP₃R isoforms, we measured the unitary

currents supported by these channels at various transmembrane potentials between +10 and –30 mV (Fig. 5). The slope of the resulting current-voltage relationship provided us with the values of single-channel conductance equal to 80.0 ± 0.3 pS ($n = 6$) for RT1, 78.0 ± 0.5 pS ($n = 4$) for RT2, and 74 ± 0.4 pS ($n = 3$) for RT3 (Fig. 5; Table 1).

InsP₃ sensitivity of mammalian InsP₃R isoforms

In the next series of experiments we studied the sensitivity of mammalian InsP₃R isoforms to InsP₃. The channel activity was recorded at pCa 6.7 in the presence of 0.5 mM ATP and in the range from 50 nM to 2 μ M of InsP₃ concentrations for InsP₃R1 and InsP₃R2 and in the range from 50 nM to 10 μ M range of InsP₃ concentrations for InsP₃R3. Because most of the experiments resulted in multichannel bilayers, the *P_o* values in each experiment were normalized to the maximal *P_o*

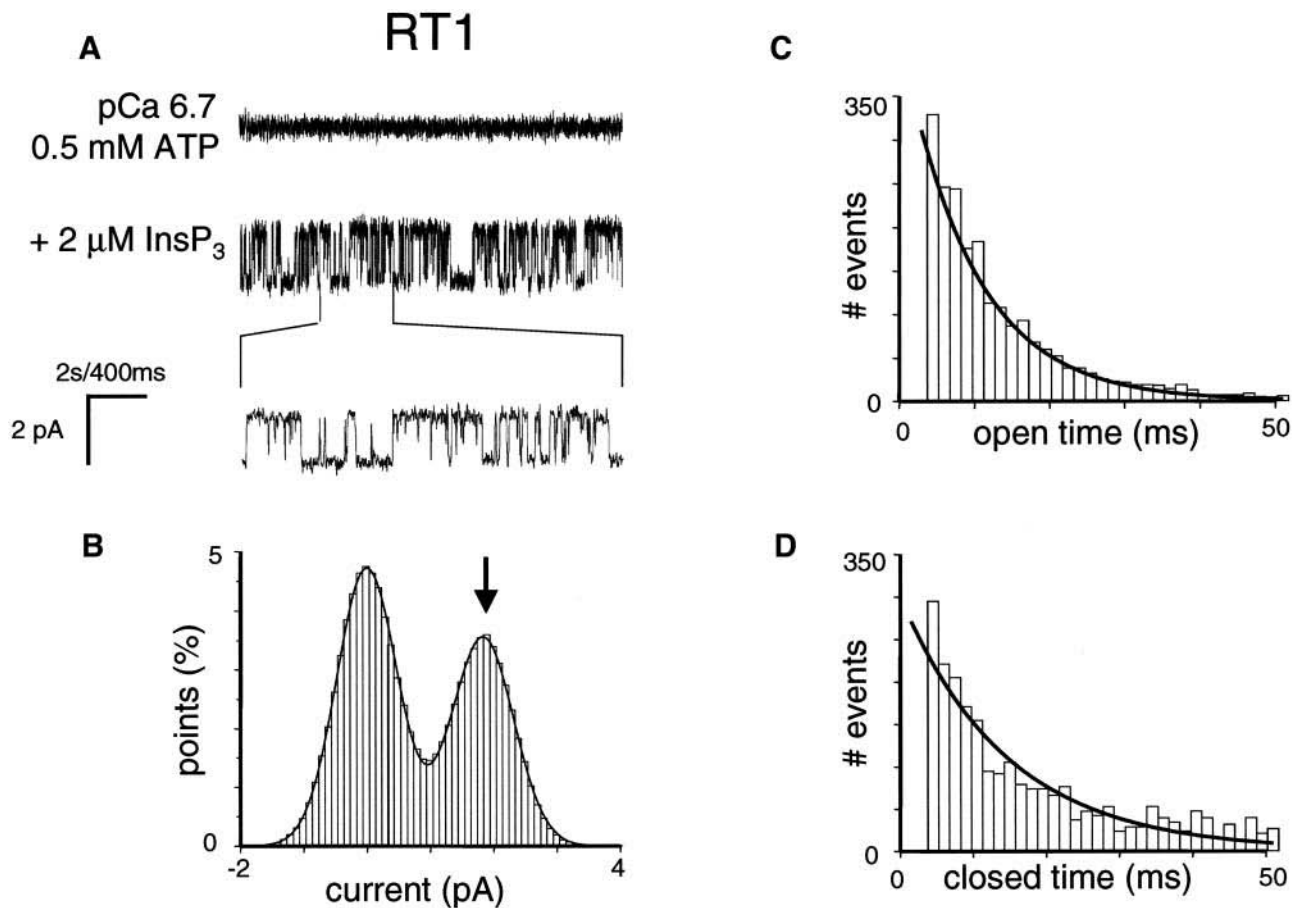


FIGURE 2 Single-channel properties of recombinant rat InsP₃R1 (RT1). (A) Single-channel records of recombinant InsP₃R1 in planar lipid bilayers. The experiments were performed at pCa 6.7 in the presence of 0.5 mM ATP (top trace). Addition of 2 μ M InsP₃ to the *cis* (cytoplasmic) side activated InsP₃R1 (middle trace). Current trace at the expanded timescale is also shown (bottom trace). (B–D) Analysis of the InsP₃R1 single-channel currents. All-points current amplitude histogram (B), open dwell time distribution (C), and closed dwell time distribution (D) are shown. The amplitude histogram (B) was fitted with a sum of two Gaussian functions corresponding to closed and open states of the InsP₃R1. The Gaussian peak corresponding to an open state of InsP₃R1 (arrow) was centered at 1.82 pA, had $\sigma = 0.49$ pA, and area 41%. Open and closed time distributions (C and D; number of events = 5000) were fitted with a single exponential function (curves) that yielded mean open time $\tau_o = 6.9$ ms and mean closed time $\tau_c = 10.1$ ms. The data from the same experiment were used for panels A–D. Similar analysis of at least three independent experiments with a single active InsP₃R1 in the bilayer was performed to generate the data for Table 1.

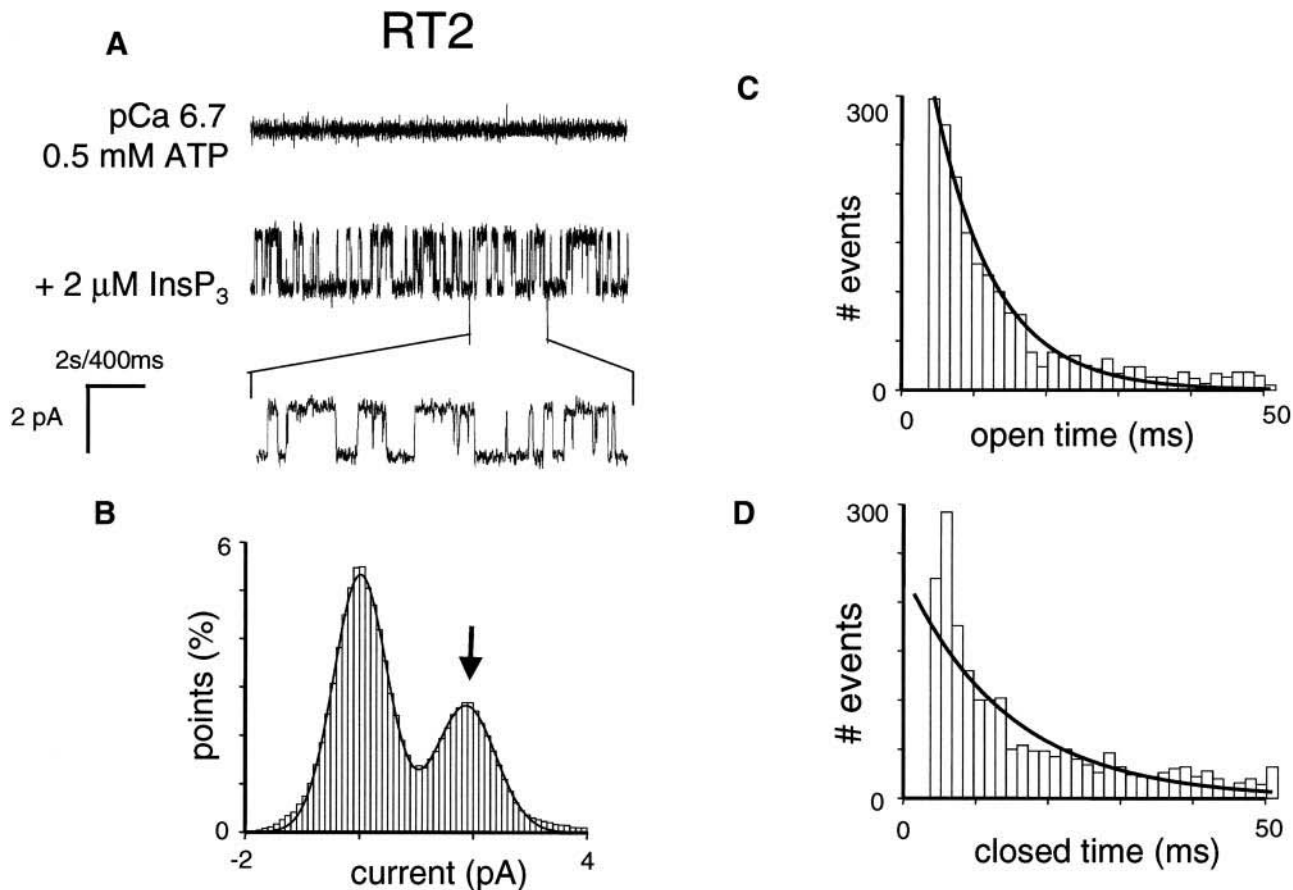


FIGURE 3 Single-channel properties of recombinant rat InsP_3R_2 (RT2). (B) Single-channel records of recombinant InsP_3R_2 in planar lipid bilayers. The experiments were performed at pCa 6.7 in the presence of 0.5 mM ATP (top trace). Addition of 2 μM InsP_3 to the *cis* (cytoplasmic) side activated InsP_3R_2 (middle trace). Current trace at the expanded timescale is also shown (bottom trace). (B–D) Analysis of the single-channel records of InsP_3R_2 was performed and analyzed as described for InsP_3R_1 in the Fig. 2 legend. The Gaussian peak corresponding to an open state of InsP_3R_2 (arrow) was centered at 1.89 pA, had $\sigma = 0.53$ pA, and area 35%. Open and closed time distributions (C and D; number of events = 5000) were fitted with a single exponential function (curves) that yielded mean open time $\tau_o = 7.6$ ms and mean closed time $\tau_c = 10.8$ ms. The data from the same experiment were used for panels A–D. Similar analysis of at least three independent experiments with a single active InsP_3R_2 in the bilayer was performed to generate the data for Table 1.

in the same experiment as described in Materials and Methods and the normalized data from different experiments with each InsP_3R isoform were averaged together for presentation and analysis. Consistent with the previous findings (Lupu et al., 1998; Tang et al., 2003; Watras et al., 1991) we found that the open probability of InsP_3R_1 was elevated with increase in InsP_3 concentration (Fig. 6, open circles). Fit to the RT1 data using Eq. 1 (Fig. 6, curve, $R^2 = 0.99$) yielded an apparent affinity $k_{\text{InsP}_3} = 0.27 \pm 0.07 \mu\text{M}$ InsP_3 (Table 2). When compared to InsP_3R_1 , InsP_3R_2 were more sensitive to activation by InsP_3 (Fig. 6, solid triangles). Fit to the RT2 data using Eq. 1 (Fig. 6, smooth curve, $R^2 = 0.98$) yielded an apparent affinity $k_{\text{InsP}_3} = 0.10 \pm 0.01 \mu\text{M}$ InsP_3 (Table 2). In contrast, InsP_3R_3 were least sensitive to activation by InsP_3 (Fig. 6, solid circles). Fit to the RT3 data using Eq. 1 (Fig. 6, curve, $R^2 = 0.98$) yielded an apparent affinity $k_{\text{InsP}_3} = 0.40 \pm 0.05 \mu\text{M}$ InsP_3 (Table 2).

Modulation of mammalian InsP_3R isoforms by ATP

InsP_3R_1 is allosterically activated by ATP (Bezprozvanny and Ehrlich, 1993; Ferris et al., 1990; Iino, 1991; Maes et al., 2000; Tu et al., 2002). Does ATP affect gating of other InsP_3R isoforms? To investigate isoform-specific modulation of InsP_3R by ATP, we measured ATP sensitivity of channel gating for the three mammalian InsP_3R isoforms in the presence of 2 μM InsP_3 at pCa 6.7 and in the range of ATP concentrations from 0 to 2.5 mM for InsP_3R_1 and from 0 to 5 mM for InsP_3R_2 and InsP_3R_3 . In agreement with the previous findings (Bezprozvanny and Ehrlich, 1993; Ferris et al., 1990; Iino 1991; Maes et al., 2000; Tu et al., 2002) we found that activity of RT1 channels was potentiated by submillimolar ATP (Fig. 7 A). In contrast, the gating of RT2 channels was ATP independent (Fig. 7 B). Activity of RT3

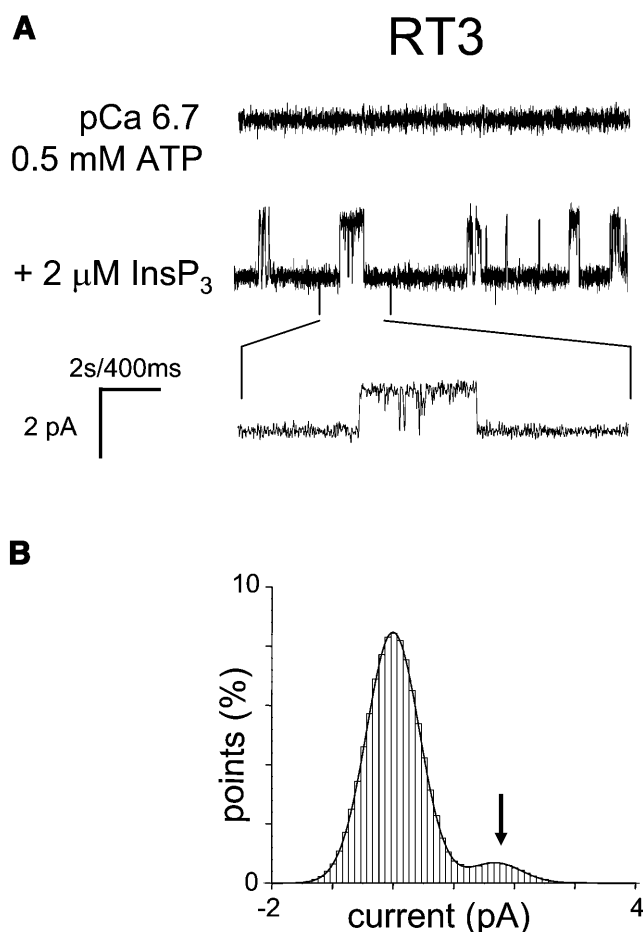


FIGURE 4 Single-channel properties of recombinant rat InsP₃R3 (RT3). (A) Single-channel records of recombinant InsP₃R3 in planar lipid bilayers. The experiments were performed at pCa 6.7 in the presence of 0.5 mM ATP (top trace). Addition of 2 μ M InsP₃ to the *cis* (cytoplasmic) side activated InsP₃R3 (middle trace). Current trace at the expanded timescale is also shown (bottom trace). (B) Amplitude histogram of InsP₃R3 was generated as described for InsP₃R1 in the Fig. 2 B legend. The Gaussian peak corresponding to an open state of InsP₃R3 (arrow) was centered at 1.76 pA, had $\sigma = 0.43$ pA, and area 7%. The data from the same experiment were used for panels A and B. Similar analysis of at least three independent experiments with a single active InsP₃R3 in the bilayer was performed to generate the data for Table 1.

channels was elevated in the presence of ATP, but ATP concentrations in excess of 2 mM were required (Fig. 7 C). Most of the experiments resulted in multichannel bilayers. Thus, to analyze obtained results quantitatively, the P_o values in each experiment were normalized to the maximal P_o in the same experiment as described in Materials and Methods and the normalized data from different experiments with each InsP₃R isoform were averaged together at each ATP concentration. Consistent with previous findings, we found that millimolar ATP increases RT1 activity approximately fivefold (Fig. 8, open circles). Fit to the RT1 data using Eq. 2 (see Materials and Methods) (Fig. 8, curve, $R^2 = 0.95$) indicated that an apparent affinity of InsP₃R1 for ATP

TABLE 1 Single-channel properties of mammalian InsP₃R isoforms

InsP ₃ R	ATP					
	(mM)	P_o (%)	i (pA)	τ_o (ms)	τ_c (ms)	γ (pS)
RT1	0.5	33 ± 5	1.9 ± 0.1	7.0 ± 0.3	9.9 ± 1.3	80.0 ± 0.3
RT2	0.5	27 ± 6	1.9 ± 0.1	7.3 ± 0.4	10.6 ± 1.6	78.0 ± 0.5
RT3	0.5	4 ± 1	1.91 ± 0.04	ND	ND	74.0 ± 0.4
	5	33 ± 9	1.8 ± 0.2	7.4 ± 1.2	9.8 ± 1.1	ND

ND, not determined.

(k_{ATP}) is equal to 0.13 ± 0.04 mM and the effects of ATP on InsP₃R1 are not cooperative ($n_{Hill} = 1.3$) (Table 2). The parameter $(P_m + P_0)/P_0$ in Table 2 reflects a degree of ATP-dependent potentiation of InsP₃R gating. Similar to RT1, RT3 activity was increased approximately sevenfold in the presence of ATP (Fig. 8, solid circles). Fit to the RT3 data using Eq. 2 (Fig. 8, curve, $R^2 = 0.98$) indicated that an apparent affinity of InsP₃R3 for ATP is equal to 2.0 ± 0.1 mM and the effects of ATP are highly cooperative ($n_{Hill} = 4.1$) (Table 2). In contrast with RT1 and RT3, gating of RT2 was ATP independent (Fig. 8, solid triangles).

Relatively low sensitivity of RT3 channels to ATP (Fig. 8, solid circles) indicated that 0.5 mM ATP used in standard recording conditions corresponds to suboptimal ATP concentration for InsP₃R3 activation. Thus, we repeated single-channel analysis of RT3-supported currents at pCa 6.7 in the presence of 2 μ M InsP₃ and 5 mM ATP (Fig. 9 A). In these conditions, P_o of InsP₃R3 was equal to $33 \pm 9\%$ ($n = 3$) (Fig. 9 B; Table 1), the size of the unitary current at 0 mV was equal to 1.8 ± 0.1 pA ($n = 3$) (Fig. 9 B; Table 1), the mean open dwell time was equal to 7 ± 1 ms ($n = 3$) (Fig. 9 C; Table 1), and the mean closed time was equal to 10 ± 1 ms ($n = 3$) (Fig. 9 D; Table 1). Thus, gating properties and open probability of RT3 channels in the presence of 5 mM ATP are similar to gating properties and open probability of RT1 and RT2 channels recorded in the presence of 0.5 mM ATP (Figs. 2, 3, and 9; Table 1).

DISCUSSION

Functional properties of mammalian InsP₃R isoforms

All three mammalian InsP₃R isoforms analyzed in our study expressed efficiently in Sf9 cells using baculoviral infection (Fig. 1) and formed InsP₃-gated channels in planar lipid bilayers (Figs. 2 A, 3 A, and 4 A). With 50 mM Ba²⁺ as a current carrier the size of the unitary current for all three mammalian InsP₃R isoforms was equal to 1.9 pA at 0 mV transmembrane potential (Figs. 2 B, 3 B, and 4 B; Table 1). The single-channel conductance for three mammalian InsP₃R isoforms was in the range 74–80 pS (Fig. 5; Table 1). In standard recording conditions (pCa 6.7, 2 μ M InsP₃, and 0.5 mM ATP on the cytosolic side of the membrane) the single-channel open probability (P_o) of the InsP₃R1 and

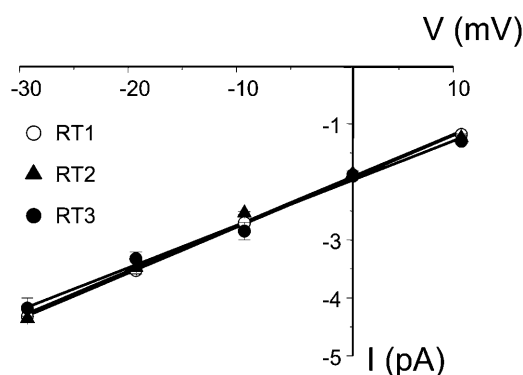


FIGURE 5 Current-voltage relationship of mammalian InsP_3R isoforms. InsP_3R currents were recorded in the planar lipid bilayers in the range of transmembrane potentials from -30 mV to $+10$ mV (*cis* versus *trans*). Single-channel current amplitude at each voltage was determined from a Gaussian fit as shown in Figs. 2 B, 3 B, and 4 B. The data for RT1 (\circ), RT2 (\blacktriangle), and RT3 (\bullet) are shown as means \pm SE ($n \geq 3$). The slope of the linear fit to the data (lines; $r = 0.99$) yielded a single-channel conductance of 80 pS for RT1, 78 pS for RT2, and 74 pS for RT3.

InsP_3R_2 channels was $\sim 30\%$ (Figs. 2 B and 3 B; Table 1), whereas P_o of InsP_3R_3 was $< 5\%$ (Fig. 4 B; Table 1). In the same recording conditions the mean open dwell time of InsP_3R_1 and InsP_3R_2 was in the range 7–8 ms (Figs. 2 C and 3 C; Table 1) and the mean closed time was ~ 10 ms (Figs. 2 D and 3 D; Table 1). When ATP dependence of InsP_3R isoforms was compared (Figs. 7 and 8; Table 2), we found that 0.5 mM ATP maximally activated InsP_3R_1 , but was not sufficient for maximal activation of InsP_3R_3 . We also found that gating of InsP_3R_2 was ATP independent. In the presence of pCa 6.7, 2 μM InsP_3 and 5 mM ATP on the cytosolic side of the membrane P_o of InsP_3R_3 was elevated to 30% (Fig. 9 B; Table 1), the mean open time was equal to 8 ms (Fig. 9 C; Table 1) and the mean closed time was equal to 10 ms (Fig. 9

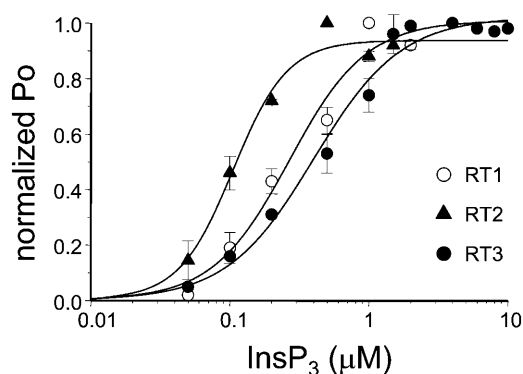


FIGURE 6 InsP_3 sensitivity of mammalian InsP_3R isoforms. The single-channel open probability (P_o) for each InsP_3R isoform was measured as a function of InsP_3 concentrations on the *cis* (cytoplasmic) side of the membrane at pCa 6.7 in the presence of 0.5 mM ATP. The normalized and averaged data (see Materials and Methods) are shown as means \pm SE ($n \geq 3$) for RT1 (\circ), RT2 (\blacktriangle), and RT3 (\bullet). The data were fitted using Eq. 1 (see Materials and Methods). The parameters of the best fit (curves) are in Table 2.

TABLE 2 InsP_3 and ATP sensitivity of mammalian InsP_3R isoforms

InsP_3R	InsP_3 dependence		ATP dependence		
	k_{InsP_3} (μM)	n_{Hill}	k_{ATP} (mM)	n_{Hill}	$(P_m + P_o)/P_o$
RT1	0.27 ± 0.07	1.6	0.13 ± 0.04	1.3	5.26
RT2	0.10 ± 0.01	2.2	N/A	N/A	N/A
RT3	0.40 ± 0.05	1.4	2.0 ± 0.1	4.1	7.14

N/A, not applicable.

Parameters k_{InsP_3} and n_{Hill} (InsP_3 dependence) were determined from the best fit to the data shown on Fig. 6 using Eq. 1, parameters k_{ATP} , n_{Hill} , P_o , and P_m (ATP dependence) were determined from the best fit to the data shown on Fig. 8 using Eq. 2.

D; Table 1). Thus, all three mammalian InsP_3R isoforms display similar maximal open probability in optimal recording conditions ($\sim 30\%$) and share common gating and conductance properties (Table 1). The similarity in conductance and gating properties is consistent with the high degree of sequence conservation in channel-forming carboxy-terminal domain of InsP_3R (Furuichi et al., 1994) and with the previous single-channel studies (Hagar et al., 1998; Mak et al., 2000; Ramos-Franco et al., 2000, 1998). In a recent study we described functional properties of recombinant *Drosophila melanogaster* InsP_3R (Dm InsP_3R) expressed in Sf9 cells by baculoviral infection and reconstituted into planar lipid bilayers (Srikanth et al., 2004). We found that Dm InsP_3R displayed conductance and gating properties remarkably similar to mammalian InsP_3R isoforms (Srikanth et al., 2004), indicating that these major functional properties of InsP_3R are conserved in evolution.

The three mammalian InsP_3R isoforms differ in sensitivity to activation by InsP_3 (Fig. 6; Table 2). The InsP_3R_2 isoform is most sensitive to activation by InsP_3 ($k_{\text{InsP}_3} = 0.10 \mu\text{M}$), followed by InsP_3R_1 ($k_{\text{InsP}_3} = 0.27 \mu\text{M}$ InsP_3), and then by InsP_3R_3 ($k_{\text{InsP}_3} = 0.40 \mu\text{M}$ InsP_3) (Fig. 6; Table 2). The differences in apparent affinities of mammalian InsP_3R isoforms to activation by InsP_3 observed in our experiments are consistent with the functional analysis of InsP_3R isoforms in DT40 cells (Miyakawa et al., 1999), and with the [^3H] InsP_3 binding (Maranto, 1994; Ramos-Franco et al., 2000; Sudhoh et al., 1991) (but see Nerou et al., 2001) and single-channel (Hagar and Ehrlich, 2000; Ramos-Franco et al., 2000) studies.

The three mammalian InsP_3R isoforms also differ in sensitivity to allosteric modulation by ATP (Figs. 7 and 8; Table 2). Search for potential ATP-binding sites with the query GYGXXG (Wierenga and Hol, 1983) reveals a presence of two potential ATP-binding sites in the InsP_3R_1 sequence $^{1773}\text{GGGGGGPG}^{1780}$ (ATPA) and $^{2015}\text{GGLGLLG}^{2021}$ (ATPB); two potential ATP-binding sites in the InsP_3R_2 sequence $^{1727}\text{GGGFTG}^{1732}$ (ATPA) and $^{1968}\text{GGLGLLG}^{1974}$ (ATPB); and a single potential ATP-binding site in the InsP_3R_3 sequence $^{1919}\text{GGLGLLG}^{1925}$ (ATPB). Previous biochemical experiments indicated that the ATPA site in the InsP_3R_1 sequence binds ATP with high affinity (Maes et al., 1999) and

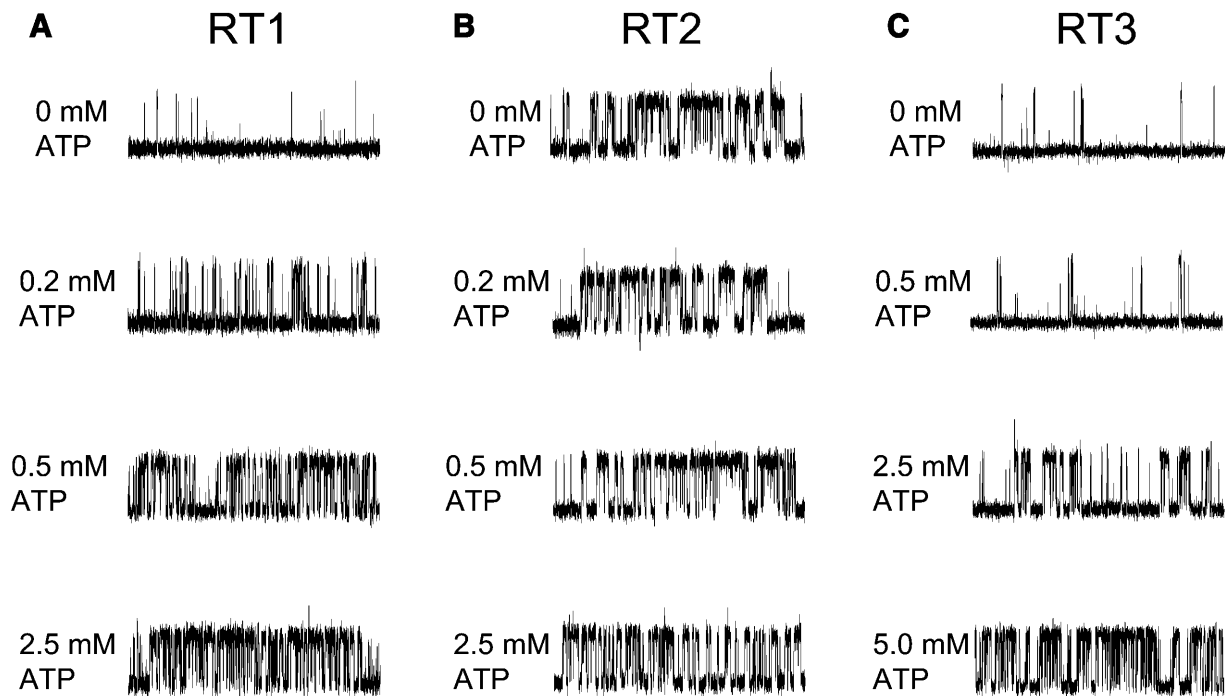


FIGURE 7 ATP sensitivity of mammalian InsP₃R isoforms. Representative current records of RT1 (A), RT2 (B), and RT3 (C) channels in the bilayers in the presence of 2 μ M InsP₃ and pCa 6.7 at concentrations of Na₂ATP as indicated on the *cis* (cytoplasmic) side of the membrane. The recordings from the same experiment are shown on each panel. Similar results were obtained in at least three experiments with each InsP₃R isoform.

ATPB sites in InsP₃R1 and InsP₃R3 bind ATP with low affinity (Maes et al., 2001, 1999). ATP-binding properties of ATPA and ATPB sites in InsP₃R2 have not been examined in biochemical experiments. We found that both InsP₃R1 and InsP₃R3 are activated approximately fivefold by ATP, whereas InsP₃R2 does not depend on ATP for maximal activation (Figs. 7 and 8). In agreement with the previous

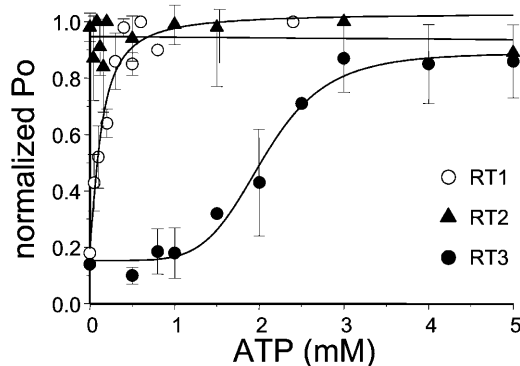


FIGURE 8 ATP modulation of mammalian InsP₃R isoforms. The single-channel open probability (P_o) for each InsP₃R isoform was measured as a function of Na₂ATP concentrations on the *cis* (cytoplasmic) side of the membrane at pCa 6.7 in the presence of 2 μ M InsP₃. The normalized and averaged data (see Materials and Methods) are shown as means \pm SE ($n \geq 3$) for RT1 (\circ), RT2 (\blacktriangle), and RT3 (\bullet). The data for RT1 and RT3 were fit by Eq. 2 (see Materials and Methods). The parameters of the best fit (curves) are in Table 2. The data for RT2 were fit by a linear regression (line).

functional studies of InsP₃R1 (Bezprozvanny and Ehrlich, 1993; Ferris et al., 1990; Iino, 1991; Maes et al., 2000; Tu et al., 2002), we found that the InsP₃R1 apparent affinity for ATP is high ($k_{ATP} = 0.13$ mM) and effects of ATP are not cooperative ($n_{Hill} = 1.3$) (Fig. 8; Table 2). Also in agreement with the previous functional studies of InsP₃R3 (Hagar and Ehrlich, 2000; Maes et al., 2000; Mak et al., 2001a; Missiaen et al., 1998), we found that the InsP₃R3 apparent affinity for ATP is low ($k_{ATP} = 2$ mM) (Fig. 8; Table 2). We also discovered that effects of ATP on InsP₃R3 are highly cooperative ($n_{Hill} = 4.1$) (Fig. 8; Table 2). High sensitivity of InsP₃R1 to modulation by ATP most likely results from the unique high-affinity ATPA site (Bezprozvanny and Ehrlich, 1993; Ferris et al., 1990; Iino, 1991; Maes et al., 2000; Tu et al., 2002). Indeed, InsP₃R1 sensitivity to modulation by ATP was greatly reduced in the InsP₃R1-*opt* mutant that lacks ATPA site (Tu et al., 2002). Low sensitivity of InsP₃R3 to modulation by ATP is consistent with low affinity of the ATPB binding site, which is likely to account for modulation of InsP₃R3 by ATP. We would like to suggest that due to low affinity and high cooperativity, InsP₃R3 regulation by ATP may be important in a physiological range of intracellular ATP concentrations (~ 2 mM). This idea is consistent with predominant InsP₃R3 expression in pancreatic β -cells (Taylor et al., 1999). We would like to propose that ATP modulation of InsP₃R3 in pancreatic β -cells may play a role in control of glucose-dependent insulin secretion. ATP modulation of InsP₃R1 is more likely to play a role in pathological

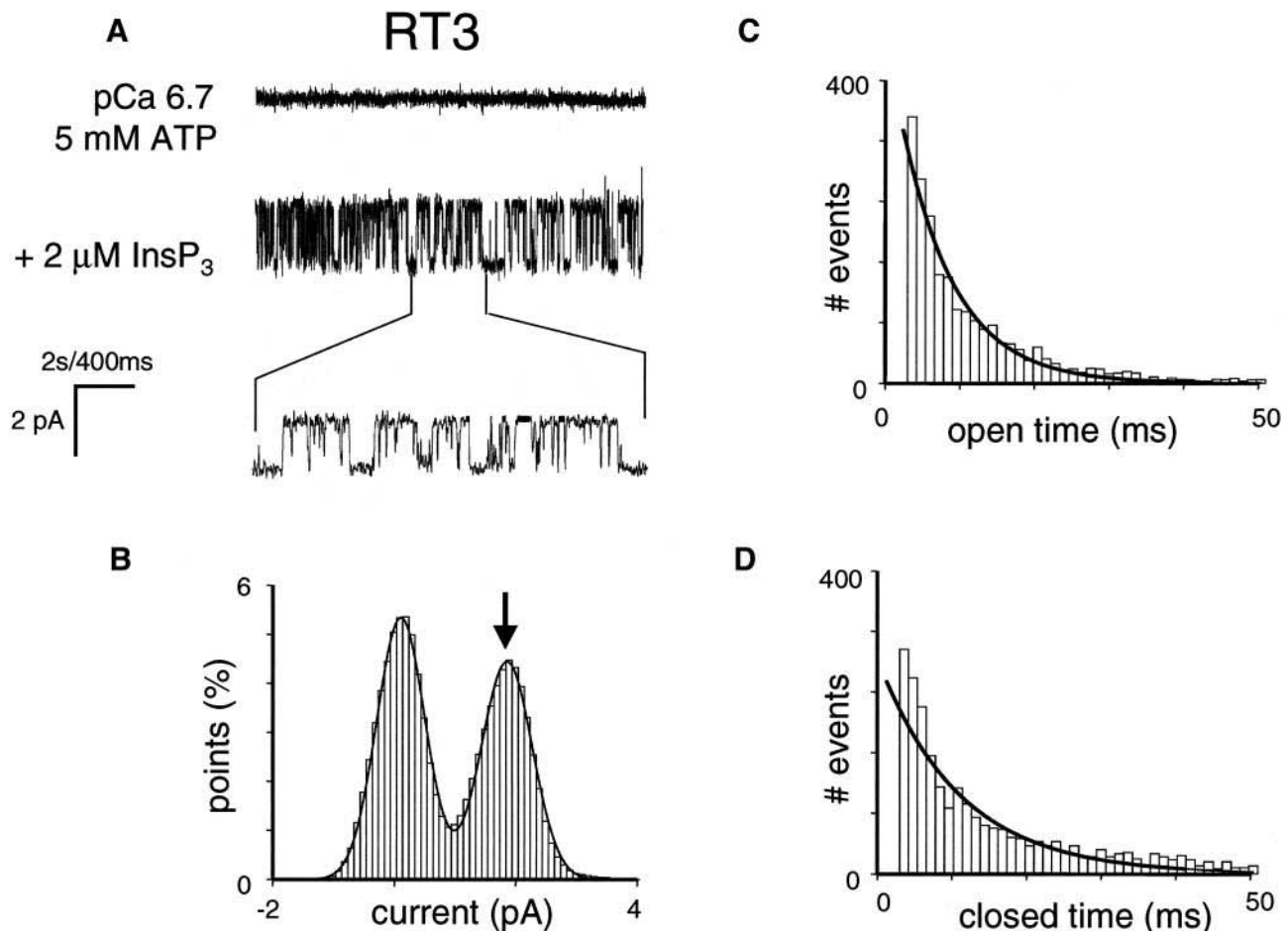


FIGURE 9 Single-channel properties of recombinant rat InsP₃R3 (RT3) at 5 mM ATP. Single-channel records of recombinant InsP₃R3 in planar lipid bilayers. The experiments were performed at pCa 6.7 in the presence of 5 mM ATP (top trace). Addition of 2 μM InsP₃ to the *cis* (cytoplasmic) side activated InsP₃R3 (middle trace). Current trace at the expanded timescale is also shown (bottom trace). (B–D) Analysis of the single-channel records of InsP₃R3 was performed and analyzed as described for InsP₃R1 in the Fig. 2 legend. The Gaussian peak corresponding to an open state of InsP₃R3 (arrow) was centered at 1.84 pA, had $\sigma = 0.34$ pA, and area 47%. Open and closed time distributions (C and D; number of events = 5000) were fitted with a single exponential function (curves) that yielded mean open time $\tau_o = 7.8$ ms and mean closed time $\tau_c = 10.2$ ms. The data from the same experiment were used for panels A–D. Similar analysis of at least three independent experiments with a single active InsP₃R3 in bilayer was performed to generate the data for Table 1.

conditions such as ischemia, when ATP concentrations can fall below 0.1 mM (Abe et al., 1987). Despite the presence of both ATPA and ATPB putative ATP-binding sites in the InsP₃R2 sequence, InsP₃R2 gating is ATP independent (Figs. 7 and 8). The ATP sensitivity of InsP₃R2 has not been previously examined in electrophysiological experiments. However, in agreement with our findings, InsP₃R2 was not modulated by ATP in Ca²⁺ flux experiments with DT40 cells (Miyakawa et al., 1999).

We are grateful to Gregory Mignery and Thomas C. Südhof for the kind gift of the rat InsP₃R1 and InsP₃R2 clones, to Dr. Graeme Bell for the kind gift of the rat InsP₃R3 clone. We thank Phyllis Foley for the administrative assistance.

This work was supported by the Welch Foundation and National Institutes of Health (R01 NS38082 to I.B.) and the Fund for Scientific Research, Flanders, Belgium (G.0210.03 to H.D.S.).

REFERENCES

- Abe, K., K. Kogure, H. Yamamoto, M. Imazawa, and K. Miyamoto. 1987. Mechanism of arachidonic acid liberation during ischemia in gerbil cerebral cortex. *J. Neurochem.* 48:503–509.
- Berridge, M. J. 1993. Inositol trisphosphate and calcium signalling. *Nature.* 361:315–325.
- Bezprozvanny, I., and B. E. Ehrlich. 1993. ATP modulates the function of inositol 1,4,5-trisphosphate-gated channels at two sites. *Neuron.* 10:1175–1184.
- Bezprozvanny, I., and B. E. Ehrlich. 1994. Inositol (1,4,5)-trisphosphate (InsP₃)-gated Ca channels from cerebellum: conduction properties for divalent cations and regulation by intraluminal calcium. *J. Gen. Physiol.* 104:821–856.
- Bezprozvanny, I., and B. E. Ehrlich. 1995. The inositol 1,4,5-trisphosphate (InsP₃) receptor. *J. Membr. Biol.* 145:205–216.
- Colquhoun, D., and A. G. Hawkes. 1983. The principles of stochastic interpretation of ion-channel mechanisms. In *Single-Channel Recording*. B. Sakmann and E. Neher, editors. Plenum Press, New York. 135–174.

- Dempster, J. 2001. *The Laboratory Computer: A Practical Guide for Neuroscientists and Physiologists*. Academic Press, New York.
- Ferris, C. D., R. L. Haganir, and S. H. Snyder. 1990. Calcium flux mediated by purified inositol 1,4,5-trisphosphate receptor in reconstituted lipid vesicles is allosterically regulated by adenine nucleotides. *Proc. Natl. Acad. Sci. USA*. 87:2147–2151.
- Furuichi, T., K. Kohda, A. Miyawaki, and K. Mikoshiba. 1994. Intracellular channels. *Curr. Opin. Neurobiol.* 4:294–303.
- Hagar, R. E., A. D. Burgstahler, M. H. Nathanson, and B. E. Ehrlich. 1998. Type III InsP₃ receptor channel stays open in the presence of increased calcium. *Nature*. 396:81–84.
- Hagar, R. E., and B. E. Ehrlich. 2000. Regulation of the type III InsP(3) receptor by InsP(3) and ATP. *Biophys. J.* 79:271–278.
- Horn, R. 1991. Estimating the number of channels in patch recordings. *Biophys. J.* 60:433–439.
- Iino, M. 1991. Effects of adenine nucleotides on inositol 1,4,5-trisphosphate-induced calcium release in vascular smooth muscle cells. *J. Gen. Physiol.* 98:681–698.
- Kaznatcheyeva, E., V. D. Lupu, and I. Bezprozvanny. 1998. Single-channel properties of inositol (1,4,5)-trisphosphate receptor heterologously expressed in HEK-293 cells. *J. Gen. Physiol.* 111:847–856.
- Lupu, V. D., E. Kaznatcheyeva, U. M. Krishna, J. R. Falck, and I. Bezprozvanny. 1998. Functional coupling of phosphatidylinositol 4,5-bisphosphate to inositol 1,4,5-trisphosphate receptor. *J. Biol. Chem.* 273:14067–14070.
- Maes, K., L. Missiaen, P. De Smet, S. Vanlingen, G. Callewaert, J. B. Parys, and H. De Smedt. 2000. Differential modulation of inositol 1,4,5-trisphosphate receptor type 1 and type 3 by ATP. *Cell Calcium*. 27:257–267.
- Maes, K., L. Missiaen, J. B. Parys, P. De Smet, I. Sienaert, E. Waelkens, G. Callewaert, and H. De Smedt. 2001. Mapping of the ATP-binding sites on inositol 1,4,5-trisphosphate receptor type 1 and type 3 homotetramers by controlled proteolysis and photoaffinity labeling. *J. Biol. Chem.* 276:3492–3497.
- Maes, K., L. Missiaen, J. B. Parys, I. Sienaert, G. Bultynck, M. Zizi, P. De Smet, R. Casteels, and H. De Smedt. 1999. Adenine-nucleotide binding sites on the inositol 1,4,5-trisphosphate receptor bind caffeine, but not adenophostin A or cyclic ADP-ribose. *Cell Calcium*. 25:143–152.
- Mak, D. O., S. McBride, and J. K. Foskett. 2001a. ATP regulation of recombinant type 3 inositol 1,4,5-trisphosphate receptor gating. *J. Gen. Physiol.* 117:447–456.
- Mak, D. O., S. McBride, and J. K. Foskett. 2001b. Regulation by Ca²⁺ and inositol 1,4,5-trisphosphate (InsP₃) of single recombinant type 3 InsP₃ receptor channels. Ca²⁺ activation uniquely distinguishes types 1 and 3 InsP₃ receptors. *J. Gen. Physiol.* 117:435–446.
- Mak, D. O., S. McBride, V. Raghuram, Y. Yue, S. K. Joseph, and J. K. Foskett. 2000. Single-channel properties in endoplasmic reticulum membrane of recombinant type 3 inositol trisphosphate receptor. *J. Gen. Physiol.* 115:241–256.
- Maranto, A. R. 1994. Primary structure, ligand binding, and localization of the human type 3 inositol 1,4,5-trisphosphate receptor expressed in intestinal epithelium. *J. Biol. Chem.* 269:1222–1230.
- Mignery, G. A., and T. C. Sudhof. 1990. The ligand binding site and transduction mechanism in the inositol-1,4,5-triphosphate receptor. *EMBO J.* 9:3893–3898.
- Miller, C. 1986. *Ion Channel Reconstitution*. C. Miller, editor. Plenum Press, New York.
- Missiaen, L., J. B. Parys, I. Sienaert, K. Maes, K. Kunzelmann, M. Takahashi, K. Tanzawa, and H. De Smedt. 1998. Functional properties of the type-3 InsP₃ receptor in 16HBE140- bronchial mucosal cells. *J. Biol. Chem.* 273:8983–8986.
- Miyakawa, T., A. Maeda, T. Yamazawa, K. Hirose, T. Kurosaki, and M. Iino. 1999. Encoding of Ca²⁺ signals by differential expression of IP₃ receptor subtypes. *EMBO J.* 18:1303–1308.
- Miyawaki, A., T. Furuichi, Y. Ryou, S. Yoshikawa, T. Nakagawa, T. Saitoh, and K. Mikoshiba. 1991. Structure-function relationships of the mouse inositol 1,4,5- trisphosphate receptor. *Proc. Natl. Acad. Sci. USA*. 88:4911–4915.
- Nerou, E. P., A. M. Riley, B. V. Potter, and C. W. Taylor. 2001. Selective recognition of inositol phosphates by subtypes of the inositol trisphosphate receptor. *Biochem. J.* 355:59–69.
- Nosyreva, E., T. Miyakawa, Z. Wang, L. Glouchankova, A. Mizushima, M. Iino, and I. Bezprozvanny. 2002. The high affinity calcium-calmodulin-binding site does not play a role in modulation of type 1 inositol (1,4,5)-trisphosphate receptor function by calcium and calmodulin. *Biochem. J.* 365:659–667.
- Ramos-Franco, J., D. Bare, S. Caenepeel, A. Nani, M. Fill, and G. Mignery. 2000. Single-channel function of recombinant type 2 inositol 1,4, 5-trisphosphate receptor. *Biophys. J.* 79:1388–1399.
- Ramos-Franco, J., M. Fill, and G. A. Mignery. 1998. Isoform-specific function of single inositol 1,4,5-trisphosphate receptor channels. *Biophys. J.* 75:834–839.
- Sakmann, B., and E. Neher. 1983. *Single-Channel Recording*. B. Sakmann and E. Neher, editors. Plenum Press, New York.
- Srikanth, S., Z. Wang, H. Tu, S. Nair, M. K. Mathew, G. Hasan, and I. Bezprozvanny. 2004. Functional properties of the *Drosophila melanogaster* inositol 1,4,5-trisphosphate receptor mutants. *Biophys. J.* 86:3634–3646.
- Sudhof, T. C., C. L. Newton, B. T. Archer, Y. A. Ushkaryov, and G. A. Mignery. 1991. Structure of a novel InsP₃ receptor. *EMBO J.* 10:3199–3206.
- Tang, T. S., H. Tu, Z. Wang, and I. Bezprozvanny. 2003. Modulation of type 1 inositol (1,4,5)-trisphosphate receptor function by protein kinase A and protein phosphatase 1α. *J. Neurosci.* 23:403–415.
- Taylor, C. W., A. A. Genazzani, and S. A. Morris. 1999. Expression of inositol trisphosphate receptors. *Cell Calcium*. 26:237–251.
- Thrower, E. C., R. E. Hagar, and B. E. Ehrlich. 2001. Regulation of Ins(1,4,5)P₃ receptor isoforms by endogenous modulators. *Trends Pharmacol. Sci.* 22:580–586.
- Tu, H., T. Miyakawa, Z. Wang, L. Glouchankova, M. Iino, and I. Bezprozvanny. 2002. Functional characterization of the type 1 inositol 1,4,5-trisphosphate receptor coupling domain SII(+/-) splice variants and the *opisthotonos* mutant form. *Biophys. J.* 82:1995–2004.
- Tu, H., E. Nosyreva, T. Miyakawa, Z. Wang, A. Mizushima, M. Iino, and I. Bezprozvanny. 2003. Functional and biochemical analysis of the type 1 inositol (1,4,5)-trisphosphate receptor calcium sensor. *Biophys. J.* 85:290–299.
- Watrass, J., I. Bezprozvanny, and B. E. Ehrlich. 1991. Inositol 1,4,5-trisphosphate-gated channels in cerebellum: presence of multiple conductance states. *J. Neurosci.* 11:3239–3245.
- Wierenga, R. K., and W. G. Hol. 1983. Predicted nucleotide-binding properties of p21 protein and its cancer-associated variant. *Nature*. 302:842–844.